Journal of Physics: Conference Series **517** (2014) 012026 doi:10.1088/1742-6596/517/1/012026

Zemax Simulations of Transition and Diffraction Radiation

T Aumeyr[1], M G Billing[2], L M Bobb[1,3], B Bolzon[3,4,5], P Karataev[1], T Lefevre[3] and S Mazzoni[3]

[1] John Adams Institute at Royal Holloway, Egham, Surrey, UK
[2] Cornell University, Ithaca, New York, USA
[3] CERN European Organisation for Nuclear Research, Geneva, Switzerland
[4] Cockcroft Institute, Worrington, Cheshire, UK
[5] University of Liverpool, Liverpool, Merseyside, UK

E-mail: Thomas.Aumeyr@rhul.ac.uk

Abstract.
Charged particle beam diagnostics is a key task in modern and future accelerator installations. The diagnostic tools are practically the "eyes" of the operators. Precision and resolution of the diagnostic equipment are crucial to define the performance. Transition and Diffraction Radiation (TR and DR) are widely used for electron beam parameter monitoring. However, the precision and resolution of those devices are determined by how well the production, transportation and detection of these phenomena are understood. This paper reports on initial simulations of TR and DR spatial characteristics. A good consistency with theory is demonstrated. Also, optical system alignment issues are discussed.

1. Introduction

Beam dynamic considerations demand very tight tolerances on most beam parameters and these in turn dictate most of the requirements for beam instrumentation [1]. Particle beams with extremely small emittances are generated in the damping rings and these must be conserved over several tens of km of beam lines. This requires a precise control of the beam position over a long distance. In most cases, the measurement of the beam size serves directly to compute the transverse beam emittance. For next generation linear colliders such as the Compact Linear Collider (CLIC) [1] or the ILC, transverse beam size measurements must have a resolution on the micron-scale. Currently, a laser-wire scanner [2] is the main candidate for non-invasive high resolution measurements. However, over a distance of more than 40 km many laser-wire monitors would be required. This is both costly and difficult to maintain.

1.1. Transition Radiation

Optical Transition Radiation (OTR) appearing when a charged particle crosses a boundary between two media with different dielectric properties has widely been used as a tool for transverse profile measurements of charged particle beams in various facilities worldwide. OTR monitors are simple, robust, and give a direct image of a two-dimensional beam profile. The resolution of the OTR monitors is normally defined as a root-mean-square of the so-called

OTR point spread function (PSF) [3]. The angular distribution can be used for beam angular divergence measurements [4].

Following the approach for calculating TR from a particle passing through a boundary between vacuum and an ideal conductor [5] and applying an ultra-relativistic approximation $\left(\theta_x, \theta_y, \gamma^{-1} \ll 1\right)$, the following equation is obtained for the vertical polarisation of the spectral-angular distribution of intensity [6]:

$$\frac{d^2W_y^{TR}}{d\omega d\Omega} = \frac{\alpha}{\pi^2}\frac{{\theta_y}^2}{\left(\gamma^{-2} + {\theta_x}^2 + {\theta_y}^2\right)^2} \tag{1}$$

Here θ_x and θ_y are the radiation observation angles measured either from the mirror reflection direction or from the particle trajectory, α is the fine structure constant and γ is the charged particle Lorentz factor. Eq. 1 is TR in the case of normal incidence, i.e. with no target tilt. However, in case of large target tilt angles and ultra-relativistic electrons, Eq. 1 can still be used for a tilted target.

1.2. Diffraction Radiation

Diffraction Radiation (DR) is produced when a relativistic charged particle moves in the vicinity of a medium [7]. The spatial-spectral properties of DR are sensitive to a range of electron beam parameters [8–10]. Furthermore, the energy loss due to DR is so small that the electron beam parameters are unchanged. Therefore DR can be used to develop non-invasive diagnostic tools.

The ODR model considers the case when a charged particle moves through a slit between two semi-planes i.e. only DR produced from the target is considered (see Fig. 1). In the case of a horizontal slit, the vertical polarisation component is sensitive to beam size [10]. Eq. 2 gives the expression for the ODR vertical polarisation component convoluted with a Gaussian distribution [10], where $t_{x,y} = \gamma\theta_{x,y}$, λ is the observation wavelength, σ_y is the rms vertical beam size, a is the target aperture size, $\overline{a_x}$ is the offset of the beam centre with respect to the centre of the slit and $\psi = \arctan\left(t_y/\sqrt{1+{t_x}^2}\right)$. This model is applicable when the transition radiation contribution from the tails of the Gaussian distribution is negligible, which means approximately $a \geq 4\sigma_y$.

$$\begin{aligned}\frac{d^2W_y^{slit}}{d\omega d\Omega} = \quad & \frac{\alpha\gamma^2}{2\pi^2}\frac{\exp\left(-\frac{2\pi a}{\gamma\lambda}\sqrt{1+{t_x}^2}\right)}{1+{t_x}^2+{t_y}^2} \\ & \times\left\{\exp\left[\frac{8\pi^2{\sigma_y}^2}{\lambda^2\gamma^2}\left(1+{t_x}^2\right)\right]\cosh\left(\frac{4\pi\overline{a_x}}{\gamma\lambda}\sqrt{1+{t_x}^2}\right) - \cos\left(\frac{2\pi a}{\gamma\lambda}t_y + 2\psi\right)\right\}\end{aligned} \tag{2}$$

This expression is valid for ultra-relativistic particles and large target tilt angles. For a slit width $a = 0$ follows considering the above approximation that $\overline{a_x} = 0$ and $\sigma_y = 0$, that Eq. 2 results in the angular distribution for OTR in Eq. 1.

2. Zemax

Optical system design is no longer a skill reserved for a few professionals. The Zemax Optical Design Program is a readily available commercial software package which integrates all the features required to conceptualise, design, optimise, analyse and tolerance virtually any optical system [11]. It is widely used in the optics industry as a standard design tool. Zemax supports two modes, geometrical ray tracing and Physical Optics Propagation (POP). Strictly speaking, geometrical ray tracing can only be used when the diffraction effect is negligible. The propagation of light is a coherent process. A wavefront traveling through free space or an optical medium, coherently interferes with itself. This is what is modelled in POP mode, using diffraction laws to propagate a wavefront through an optical system interface by interface.

In POP mode, the entire beam array must be stored in computer memory at once contrary to the ray tracing mode. Therefore, a large quantity of RAM is needed when using the POP mode for large sampling arrays and because imaging systems require large sampling to accurately model aberrations. The wavefront is modelled using an array of discretely sampled points, analogous to the discrete sampling using rays for geometric optics analysis. Each point in the array stores complex amplitude information about the beam. The entire array is then propagated in free space between optical interfaces. At each optical interface, a transfer function is computed which propagates the beam from one side of the optical surface to the other, using either Fresnel diffraction propagation or an angular spectrum propagation algorithm [12, 13]. Zemax automatically chooses the algorithm that yields the highest numerical accuracy. The diffraction propagation algorithms yield correct results for any propagation distance, for any arbitrary source and can account for any surface aperture, including User Defined Apertures (UDAs).

2.1. Physical Optics Propagation algorithm

Zemax propagates any spatial complex electric field defined by a 2D matrix. The electric field is represented in three dimensions as

$$\boldsymbol{E}(x, y, z) = E_x\hat{x} + E_y\hat{y} + E_z\hat{z}, \tag{3}$$

where all $\boldsymbol{E}$ values are complex and $\hat{x}$, $\hat{y}$ and $\hat{z}$ are the Cartesian unit vectors. Because the beam is propagating along the local z direction, the first approximation made is to neglect the E_z component. By keeping track of the electric field components along both the x and y axes, polarisation effects can be studied, such as transmission and reflection losses, polarisation aberrations and the polarisation state of the beam. If polarisation effects are not required, the x component of the field can be ignored, thus speeding up the computations.

For a beam with a radius R propagating over a distance Z, the Fresnel number N_F is defined by

$$N_F = \frac{2}{\lambda}\left(\sqrt{Z^2 + R^2} - Z\right). \tag{4}$$

Assuming $Z \gg R$, this expression reduces to

$$N_F = \frac{R^2}{\lambda Z}. \tag{5}$$

The Fresnel number is equal to the number of Fresnel rings on the source plane that can be seen from any point on the detection plane:

- Fraunhofer diffraction (far field): $N_F = 0$
- Fresnel diffraction (pre-wave zone if $R > \gamma\lambda$): $0 < N_F < 1$
- Angular Spectrum Propagation (near field): $N_F > 1$

The decision on the Fresnel numbers, and thus on the algorithms used by Zemax, is based on a pilot beam. By default, the pilot beam is an ideal Gaussian beam, with a waist, beam size, phase radius and relative z position. The initial parameters may be generated by fitting the Gaussian beam equations to the initial distribution. However, it is also possible to define a pilot beam if the electric field defined at the source is a non-Gaussian beam.

In any case, the pilot beam is then propagated from interface to interface. At each interface, new beam parameters, such as the new waist, phase radius, or position are computed. The properties of the pilot beam are then used to determine if the actual distribution is inside or outside the Rayleigh range, and what propagation algorithms are appropriate.

2.2. Defining the source

Several types of beam are already predefined as source in POP: Gaussian Waist, Gaussian Angle, Gaussian Size+Angle, Top Hat, File, Windows Dynamic Link Library (DLL) or Multimode. Moreover, any source of light can be provided by the user in POP. The user has to define, among others, the spatial distribution of the complex electric field of the source either in a *Beam File* or in a DLL. In both cases, the parameters of the pilot beam have to be defined. These are the pilot beam waist, the Rayleigh distance and the pilot position, both in x and y directions.

The most practical way to define a source using an external program, is to compute the initial electric field into a Windows Dynamic Link Library (DLL). Sample DLLs with source code are provided with Zemax. These examples are of great help to see how the DLL should be written to properly define the source amplitude and phase. The instructions to compile such a C source file into a DLL can be found on the Zemax support website.

With a DLL, it is possible to define between zero and eight user defined data values as input parameters in the computation of the beam properties. This is particularly useful when the electric field is defined by an equation, whose parameters have to be changed by the user from one simulation to the next (e.g. particle energy, observation wavelength, etc.).

Starting with the example C source file provided with Zemax, the only changes that had to be applied are the equation of the electric field, the user-defined data values and the pilot beam parameters which were set to 0. The OTR electric field programmed in the C source file is the approximation of the electric field for y polarisation component induced by a single electron on a target surface [14], based on the solution of Maxwell equations for a field of a charged particle moving in free space. Up to a constant it is (see [5])

$$E_{y,real} = const \cdot \frac{y}{\sqrt{x^2+y^2}} \left[\frac{2\pi}{\gamma\lambda} K_1\left(\frac{2\pi}{\gamma\lambda}\sqrt{x^2+y^2}\right) - \frac{J_0\left(\frac{2\pi}{\lambda}\sqrt{x^2+y^2}\right)}{\sqrt{x^2+y^2}} \right] \qquad (6)$$

$$E_{y,imag} = 0.$$

Here x and y are two orthogonal coordinates of the target measured from the point of electron incidence, γ is the charged particle Lorentz factor, λ is the radiation wavelength, K_1 is the first order modified Bessel function, J_0 is the zero order Bessel function.

According to the Fresnel-Huygens principle, the field of the particles reflected off the target surface represents the radiation field. For TR the entire field is reflected and propagates towards the observation plane. In case of DR, only a part of the field is reflected, depending on the target geometry.

3. Simulations

3.1. Comparing simulations with theory

In Fig. 2, the ODR angular distribution for various slit sizes at the detector plane created by a single electron passing through a source with a 1 mm vertical slit ($\gamma = 4110, \lambda = 400$ nm) is shown. This corresponds to the experimental conditions at the ODR monitor at the Cornell Electron Storage Ring (CesrTA) [15]. The distance between the source and detector plane was set to 100 m to ensure the angular distribution is fully defined. Comparing with the analytical expression given in Eq. 2, a nearly perfect agreement can be observed.

At the Accelerator Test Facility (ATF), the OTR monitor uses an observation wavelength of $\lambda = 550$ nm for a beam Lorentz factor of $\gamma = 2500$ [10]. The far-field requirement for OTR is $L \gg \frac{\gamma^2\lambda}{2\pi} = 0.55$ m, therefore the distance of 100 m between source and detector plane was more than enough to achieve a perfect consistency. The size of the source was $r_{max} = 10 \cdot \frac{\gamma\lambda}{2\pi} = 2.188$ mm to fulfil an infinite target approximation. Fig. 3 shows the effect on

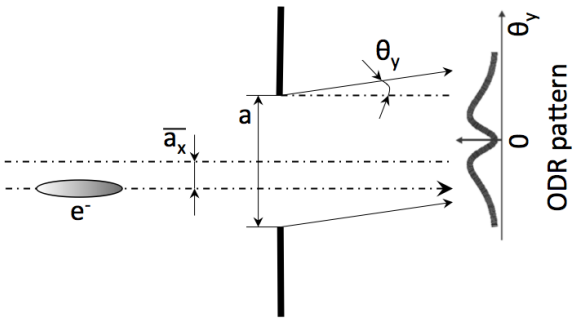

Figure 1: Geometry of the ODR production.

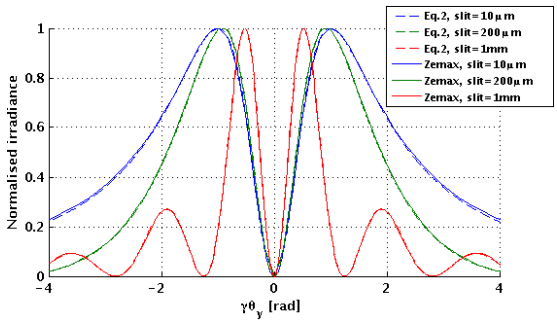

Figure 2: ODR angular distribution for various slit sizes compared with theory.

the angular distribution when moving the detector plane from the near-field into the far-field. The distribution was simulated at three different distances from the source - $\frac{\gamma^2\lambda}{2\pi}$, $2 \cdot \frac{\gamma^2\lambda}{2\pi}$ and $10 \cdot \frac{\gamma^2\lambda}{2\pi}$. This figure is in excellent agreement with analytical calculations [16].

The far-field condition for the parameters for the ODR monitor at CesrTA is fulfilled for a distance $L \gg \frac{\gamma^2\lambda}{2\pi} = 1.08$ m. The size of the simulated source was $r_{max} = 10 \cdot \frac{\gamma\lambda}{2\pi} = 2.617$ mm. As in the OTR case, Fig. 4 shows the effect on the angular distribution when moving the detector plane from the near-field into the far-field, this time using a slit width of 300 µm. The distribution was again simulated at three different distances from the source.

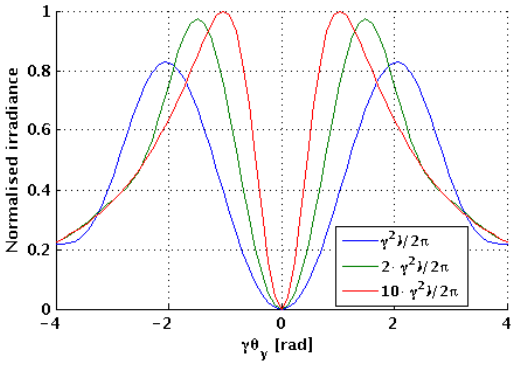

Figure 3: OTR angular distribution for various distances from source to image.

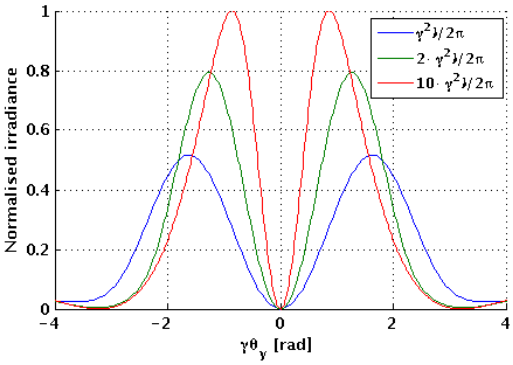

Figure 4: ODR angular distribution for various distances from source to image.

3.2. Optimisation and alignment of the optical system

After establishing agreement between simulation and theory when propagating in free space, optical systems can be optimised and studied with respect to misalignment. Inserting a bi-convex lens and putting the image plane in the back focal plane (BFP) of the lens, a full angular distribution can be established in the near-field. Fig. 5 shows the ODR angular distributions for various positions of the image plane. It can be seen that the ODR angular distribution is very sensitive to distances away from the focal plane. The detector must therefore be exactly in the back focal plane (BFP). The same simulation parameters as above were used. Zemax has a built-in lens catalog, including most commercially available lenses. The position of BFP of the biconvex chosen for the ODR optical system at CesrTA is 326.63 mm.

Simulating the ODR angular distribution when tilting the biconvex lens can be seen in Fig. 6. To compare the change in the angular distribution pattern, the distributions are referenced to a reference sphere and therefore centred at $\theta_y = 0$.

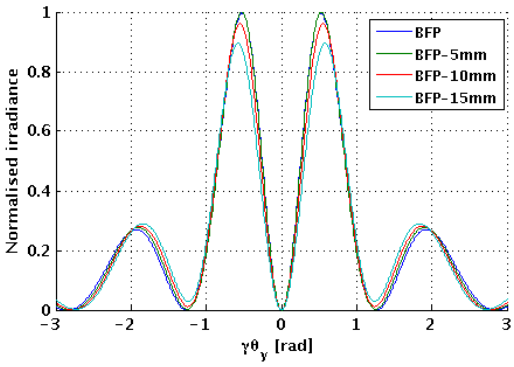

Figure 5: ODR angular distribution for various positions of the image plane (BFP is the position of the back focal plane).

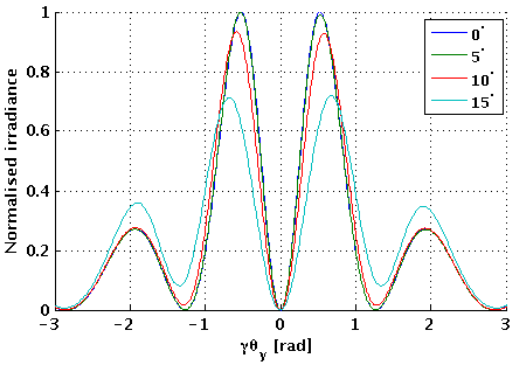

Figure 6: ODR angular distribution for various tilts about the y-axis.

4. Conclusion and future prospects

With assumptions similar to theoretical boundary conditions, Zemax simulations of OTR and ODR agree with the analytical expressions. The next step is to improve the simulation further with including a tilt angle in the incident electric fields to enable simulating a tilted target. With this, agreement can also be achieved for low energies.

Furthermore, simulations will be done applying a finite beam size. This can be achieved by displacing the single particle with respect to the optical axis across the transversal profile. The resulting angular pattern for each step can then be weighted and summed up. After comparing this with analytical equations, the software will have been proven useful for studies of any type of optical system using OTR or ODR. Introducing an off-axis incident field or even an arbitrarily shaped aperture does not slow down the Zemax simulations noticeably and is therefore the preferable method.

This will enable simulations of all misalignment errors and optimisation of a real optical system to be implemented in a real diagnostic station (including viewports, polarisers, filters, etc.). Field depth studies can then be done as well as investigations on the behaviour of the OTR PSF in real optical setups. Also, beam divergence and energy spread will be included to simulate realistic beam properties.

References

[1] CLIC Conceptual Design Report, to be published in 2012, `http://clic-study.org/accelerator/CLIC-ConceptDesignRep.php`
[2] S.T. Boogert et al., Phys. Rev. ST Accel. Beams 13 (2010) 122801.
[3] M. Castellano and V.A. Verzilov, Phys. Rev. ST Accel. Beams 6 (1998) 062801.
[4] R.B. Fiorito et al., Phys. Rev. ST Accel. Beams 9 (2006) 052802.
[5] M.L. Ter-Mikaelian, *High Energy Electromagnetic Processes in Condensed Media*, Wiley, New York (1972).
[6] A. Potylitsyn, Nucl. Inst. and Meth. B 145 (1998) 169-179.
[7] A. Potylitsyn et al., *Diffraction Radiation from Relativistic Particles*, Springer Tracts Mod.Phys. 239 (2011) 1-260
[8] M.Castellano, Nucl. Inst. and Meth. A 394 (1997) 275-280.
[9] J. Urakawa et al., Nucl. Inst. and Meth. A 472 (2001) 309-317.
[10] P. Karataev et al., Phys. Rev. Lett. 93 (2004) 244802.
[11] Zemax 13, Optical Design Program, *Users Manual*, February 20, 2013.
[12] J.W. Goodman, *Introduction to Fourier Optics*, McGraw-Hill, New York (1968).
[13] G.N. Lawrence, *Optical Modeling*, Applied Optics and Optical Engineering 11, Academic, New York (1992).
[14] M. Castellano et al., Nucl. Inst. and Meth. A 435 (1999) 297.
[15] D. Rubin et al., Proc. of PAC2009, Vancouver, Canada, WE6PFP103, p. 2751.
[16] P.V. Karataev, Phys. Lett. A 345 (2005) p. 428-438.